



GLOBAL JOURNAL OF RESEARCHES IN ENGINEERING: F  
ELECTRICAL AND ELECTRONICS ENGINEERING  
Volume 16 Issue 2 Version 1.0 Year 2016  
Type: Double Blind Peer Reviewed International Research Journal  
Publisher: Global Journals Inc. (USA)  
Online ISSN: 2249-4596 & Print ISSN: 0975-5861

## Control Strategies of a Neuro-Fuzzy Controlled Grid Connected Hybrid PV/PEMFC/Battery

By T. Praveen Kumar, N. Subrahmanyam & M. Sydulu

*National Institute of Technology, India*

**Abstract-** This paper depicts power control strategies of a neuro-fuzzy controlled grid connected hybrid photovoltaic and proton exchange membrane fuel cell distributed generation system with battery as energy storage device. The essential source of energy for the hybrid distributed generation system is from photovoltaic cell and proton exchange membrane fuel cell and the battery acts as a complementary source of energy. The hybrid distributed generation system is connected to a grid through power electronic interfacing devices. A Matlab/Simulink model is developed for the grid connected hybrid distributed generation system, neuro-fuzzy controlled power electronic DC/DC and DC/AC converters to control the flow of power on both sides. Likewise we extended our work so as to distribute the power between power sources, the neuro-fuzzy power controller has been developed. Simulation results are presented to demonstrate the effectiveness and capability of proposed control strategy.

**Keywords:** *shunt active power filters, total harmonic distortion, power conversion, power drives.*

**GJRE-F Classification :** *FOR Code: 080108*



*Strictly as per the compliance and regulations of :*



# Control Strategies of a Neuro-Fuzzy Controlled Grid Connected Hybrid PV/PEMFC/Battery

T. Praveen Kumar <sup>α</sup>, N. Subrahmanyam <sup>σ</sup> & M. Sydulu <sup>ρ</sup>

**Abstract-** This paper depicts power control strategies of a neuro-fuzzy controlled grid connected hybrid photovoltaic and proton exchange membrane fuel cell distributed generation system with battery as energy storage device. The essential source of energy for the hybrid distributed generation system is from photovoltaic cell and proton exchange membrane fuel cell and the battery acts as a complementary source of energy. The hybrid distributed generation system is connected to a grid through power electronic interfacing devices. A Matlab/Simulink model is developed for the grid connected hybrid distributed generation system, neuro-fuzzy controlled power electronic DC/DC and DC/AC converters to control the flow of power on both sides. Likewise we extended our work so as to distribute the power between power sources, the neuro-fuzzy power controller has been developed. Simulation results are presented to demonstrate the effectiveness and capability of proposed control strategy.

**Keywords:** shunt active power filters, total harmonic distortion, power conversion, power drives.

## I. INTRODUCTION

The penetration level of green and renewable energy sources/distributed generation units are expected to grow in the near future as there is a probability of rundown conventional fuels for power generation. The distributed generation is classified as renewable and non-renewable. The distributed generation sources such as Fuel cells, Wind and Solar energy are increasing daily due to increase in demand for electrical power [1]. These energy sources are environmental friendly, reduces transmission and distribution losses, peak load shaving, can be used as backup sources and etc. Fuel cell is a promising device as it is efficient, modular and can be placed at any site for improving system efficiency [2] but it has slow start-up response. Solar energy is an important renewable energy source [3] but the intermittent nature of this technology is a major issue. The accessibility of energy is driven by climate and cell temperature however not on the loads of the systems. This innovation can be marked as irregular and typically PV array utilizes a Maximum Power Point Tracking (MPPT) (MPPT) strategy to consistently convey the most highest power to the load when there are variations in irradiation and temperature [4]. Because of the intermittent nature of PV array it

becomes an uncontrollable source. In order to overcome the drawbacks with the slow start-up of fuel cells and intermittent nature of PV cell a neuro-fuzzy controlled grid associated hybrid photovoltaic as well as proton exchange membrane fuel cell (PEMFC) distributed generation system with battery as energy storage is suggested in this paper.

## II. SYSTEM MODELING

Fig. 1 shows the block diagram of the HRPS (Hybrid Renewable Power Sources) proposed in this paper that connected to main grid in Point Common Coupling (PCC). So by above discussions two mathematical models recitation the dynamic behavior and each of these constituents are given below.

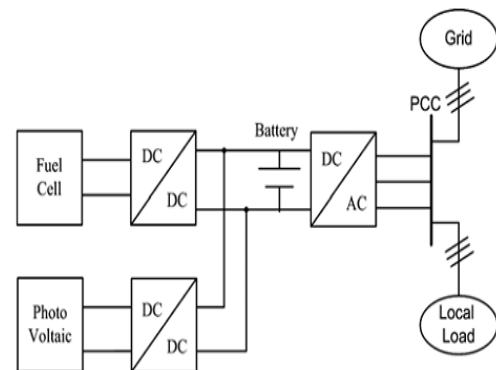


Fig-1 : Block Diagram of Grid connected Hybrid system

### a) Proton Exchange Membrane Fuel Cell Model

A fuel cell functions like a battery by transforming the chemical energy into electrical energy, but it differs from a battery in that as long as the hydrogen and oxygen is supplied it will produce DC electricity continuously. Fuel cells play a vital role in distributed generation because of their advantages such as high efficiency, no contamination gasses and particular structure adaptability.

The Nernst's mathematical statement and Ohm's law oversee the normal voltage size of the fuel cell stack. The subsequent mathematical statement representations the voltage of the fuel cell stack:

$$V_{fc} = N_0(E_0 + \frac{RT}{2F} (\log \left( \frac{P_{H_2} P_{O_2}^{0.5}}{P_{H_2O}} \right))) - R_{int} I \quad (1)$$

Author <sup>α</sup>: Research Scholar, Dept. of Electrical Engineering, National Institute of Technology, Warangal, Telangana, India.

Author <sup>σ</sup> <sup>ρ</sup>: Professor, Dept. of Electrical Engineering, National Institute of Technology, Warangal, Telangana, India.

e-mail: praveen3564@gmail.com

Where:

$N_0$  is the number of cells connected in series;  
 $R_{int}$  is the internal resistance of fuel cell stack [ $\Omega$ ]  
 $E_0$  is the voltage related with the reaction free energy;  
 $R$  is the universal gas constant;  
 $T$  is the temperature;  
 $I$  is the current of the fuel cell stack;  
 $F$  is the Faraday's constant.

$P_{H_2}, P_{H_2O}, P_{O_2}$  are dictated by the accompanying differential equations.

$$\begin{aligned}
 P_{H_2} &= -\frac{1}{t_{H_2}}(P_{H_2} + \frac{1}{K_{H_2}}(q_{H_2}^{in} - 2K_r I_{fc})) \\
 P_{H_2O} &= -\frac{1}{t_{H_2O}}(P_{H_2O} + \frac{2}{K_{H_2O}}K_r I_{fc}) \\
 P_{O_2} &= -\frac{1}{t_{O_2}}(P_{O_2} + \frac{1}{K_{O_2}}(q_{O_2}^{in} - K_r I_{fc}))
 \end{aligned}
 \tag{2}$$

Where,  $q_{H_2}^{in}$  and  $q_{O_2}^{in}$  are the molar flow of hydrogen and oxygen and where the  $K_r$  constant is well-defined by the relation between the rate of reactant hydrogen and the fuel cell current:

$$q_{H_2}^r = \frac{N_0 I}{2F} = 2K_r I \tag{3}$$

Besides, a straightforward model of reformer that creates hydrogen through methane has been deliberated and the model is second-order transfer function. So therefore its mathematical form can be written as follows:

$$\frac{q_{H_2}}{q_{metanne}} = \frac{CV}{\tau_1 \tau_2 S^2 + (\tau_1 + \tau_2)S + 1}$$

Where  $q_{metanne}$  is methane flow rate [kmol/sec];  
 $CV$  is conversion factor [kmol of hydrogen per kmol of methane];

$\tau_1, \tau_2$  are reformer time constants [sec].

b) Photovoltaic Model (PV)

The equivalent circuit shown in Fig.2 is a one diode model of a solar cell which consists of a diode and a current source connected in parallel with a series resistance  $R_s$ . The current source feeds the photocurrent  $I_{ph}$ , which is directly proportional to solar irradiance  $G$ . By referring manufacturer's data sheet, the two main parameters used to describe a PV cell are open circuit voltage and another is its short circuit current.

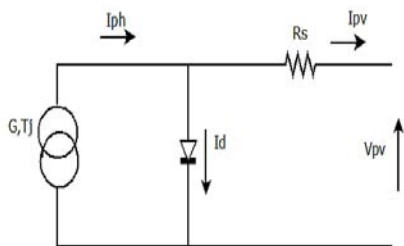


Fig.2 : Equivalent solar cell model with  $R_s$

The mathematical model [3] of PV cell can be expressed as

$$I_{pv} = I_{ph} - I_0 \left[ \exp q \left( \frac{V_{pv} + I_{pv} \cdot R_s}{AKT} \right) - 1 \right] \tag{4}$$

Since Photocurrent  $I_{ph}$  is directly proportional to solar radiation  $G$ .

$$I_{ph}(G) = I_{sc} \frac{G}{G_{ref}} \tag{5}$$

The short-circuit current  $I_{sc}$  of solar cell depends linearly on cell temperature.

$$I_{sc}(T_j) = I_{sc} [1 + \Delta I_{sc} (T_j - T_{jref})]$$

$$I_{ph}(G, T_j) = I_{scs} \frac{G}{G_{ref}} [1 + \Delta I_{sc} (T_j - T_{jref})] \tag{6}$$

$I_0$  also depends on solar irradiation as well as cell temperature and that can be mathematically expressed as follows

$$I_0(G, T_j) = \frac{I_{ph}(G, T_j)}{e \left( \frac{V_{oc}(T_j)}{V_t(T_j)} \right) - 1} \tag{7}$$

In the writing numerous MPPT strategies are accessible, for instance, incremental conductance (INC), consistent voltage (CV), and perturbation and observation (P&O). Therefore P&O strategy has been generally utilized in view of its basic input structure and less measured parameters. The panel voltage is purposely intentionally agitated (expanded or diminished) then the power is contrasted with the power got before to disturbance. In particular, if the power panel is increased because of the unsettling influence, the accompanying disturbance will be made in the same course and if the power diminishes, the new perturbation is made in the opposite direction. But the demerit with P & O is the output power is oscillating in nature. Because of this reason we use the Fuzzy MPPT technique to deliver the maximum power and to eliminate perturbations in the output power.

c) Fuzzy MPPT Control

The inputs to the fuzzy MPPT control can be measured or computed from the voltage and current of solar panel. The control rules are indicated in [4] with  $\Delta P_{pv}$  and  $\Delta V_{pv}$  as inputs and  $\Delta V_{pvref}$  as the output. The membership functions of input and output variables in which membership functions of input variables  $\Delta P_{pv}$  and  $\Delta V_{pv}$  are triangular and has seven fuzzy subsets. Seven fuzzy subsets are considered for membership functions of the output variable  $\Delta V_{pvref}$ . These input and output variables are expressed in terms of linguistic variables (such as BN (big negative), MN (Medium negative), SN (small negative), Z (zero), SP (small positive), MP (medium positive), and BP (big positive)).

d) Battery Modelling

The battery is a device which stores energy in electro chemical form. Battery is used as energy storage device in wide range of applications like hybrid electric vehicles and hybrid power systems. In this paper, the battery energy storage is combined with hybrid PV/PEMFC distributed generation system. The battery model considered in this paper is shown in fig.3. The battery model used is based on voltage model proposed by Shepherd [4].

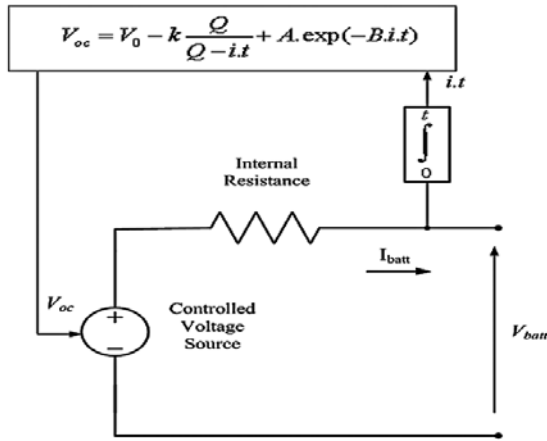


Fig. 3 : Battery Model

e) DC/DC Boost Converter Model

The role of boost DC/DC converters is to deliver power to the user in appropriate form at high efficiency. Generally the Power electronic converters are desirable in PV and fuel cell systems to transform DC voltage to the prerequisite values. Fig. 4 shows the DC/DC converter model.

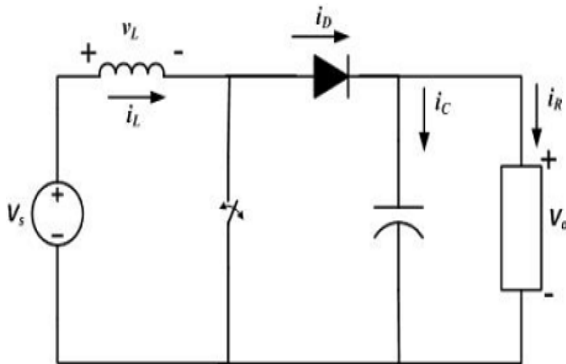


Fig. 4 : Boost DC/DC Converter Model.

As depicted above boost converter is defined by the following two nonlinear state space averaged equations [7]:

$$\begin{aligned} \frac{di_L}{dt} &= -\frac{R_L}{L} - \left(\frac{1-d}{L}\right)V_0 + \frac{1}{L}V_s \\ \frac{dV_C}{dt} &= \left(\frac{1-d}{C}\right)i_L + \frac{i_R}{C} \end{aligned} \quad (8)$$

where “d” is the duty cycle of the switching device, “U” is the input voltage, “i<sub>L</sub>” is the inductor

current, “V<sub>c</sub>” is the output voltage and “i<sub>o</sub>” is the output current.

f) DC-AC Converter Model

Converter (VSC) is shown in Fig. 5. To reduce harmonics, LCL filter is connected between the converter and also at the grid side [6]. So therefore the dynamic model of the three-phase VSC is represented in

$$\begin{aligned} \frac{di_{1k}}{dt} &= -\frac{R_1}{L_1}i_{1k} + \frac{1}{L_1}(V_{1k} - V_{ck}) \\ \frac{di_{2k}}{dt} &= -\frac{R_2}{L_2}i_{2k} + \frac{1}{L_1}(V_{ck} - V_{sk}) \\ C_f \frac{dV_{ck}}{dt} &= i_{1k} - i_{2k} \end{aligned} \quad (9)$$

Where k={a, b, c}

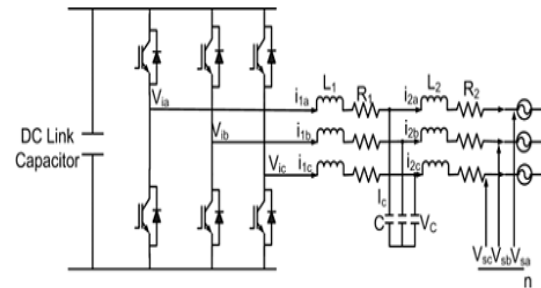


Fig.5 : DC/ AC Three Phase Inverter

### III. POWER CONTROL STRATEGIES OF HYBRID SYSTEM

By above discussions the Power flow control from hybrid power sources to local AC bus and to/from storage devices is required to keep up power balance at all times while fulfilling the the active and reactive power demanded by the load. Eq.(13) gives power balance expressions that should be satisfied together at the DC-link and at the P<sub>CC</sub> all the time.

The rate and magnitude of fuel cell power P<sub>FC</sub> and rate, sign and magnitude of battery power P<sub>Batt</sub> depend on the magnitude and how fast the load changes.

$$\begin{aligned} P_{DG} &= P_{PV} + P_{PC} + P_{Batt} \\ P_{Load} &= P_{DG} + P_{Grid} \\ Q_{Load} &= Q_{DG} + Q_{Grid} \end{aligned} \quad (10)$$

According to the control strategy proposed in this paper, P<sub>Load</sub> and Q<sub>Load</sub> are made equal to P<sub>ref</sub> and Q<sub>ref</sub> so that the hybrid power system output shadows the load demand only under normal loading conditions also P<sub>Grid</sub> and Q<sub>Grid</sub> are seems to be zero. So if the local load demand surpasses the hybrid power system capacity, then remaining of the power is supplied from the grid side. Fig. 6 shows the overall structure of the control strategy.

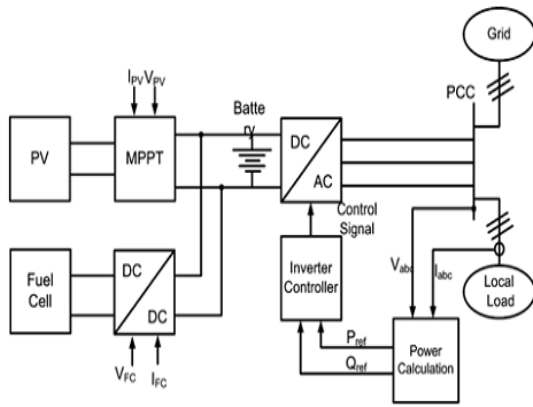


Fig. 6 : Overall system control structure.

Hence the control strategy also retains the DC-link/battery voltage within a band about the nominal DC-link voltage to have the inverter in synchronism with the grid. The following differential equation for DC link power balance is given:

$$C_{dc} v_{dc} \frac{dv_{dc}}{dt} = P_{FC} + P_{PV} + P_{Batt} - P_{Grid} \quad (11)$$

Moreover, to meet the requirements of power balance in DC link it is significant to consider the dynamic limitations of fuel cell power. In this case, the fuel cell power could not change rapidly and the fuel cell controller with DCDC converter should regulate the operating point of fuel cell. But the amount of power that should be absorbed by battery energy storage in order to balance the power in DC link is significant and also it is greatly influenced by DC link energy, where its energy measurement is supported with the help of the following calculation:

$$E_{dc}(k) = \left(\frac{1}{2}\right) C_{dc} V_{dc}^2(k) \quad (12)$$

In this paper, a power flow control structure has been established for hybrid power sources during voltage sag. It is based on Fuzzy Logic Control (FLC) strategy that determines the battery energy storage power according to the following inputs:

$$e(k) = E_{dc-ref}(k) - E_{dc}(k) \\ \Delta e(k) = e(k) - e(k-1) \quad (13)$$

where  $E_{dc-ref}$  is the reference dc link energy which is calculated by reference dc link voltage. Subsequently, it is crucial to outline powerful and stable control technique to ensure the stability of the dc link of hybrid system. For this purpose, a fuzzy neural control strategy is developed [8].

#### IV. NEURO-FUZZY CONTROL STRATEGY

In this paper a neuro-fuzzy control strategy, for each of the input, four fuzzy subsets have been employed. These are ZE (zero), L (low), M (medium) and H (high). So for all of these fuzzy sets, a gaussian membership function has been used. As each of the two

inputs has four subsets, there are altogether 16 control rules in the neuro-fuzzy logic controller.

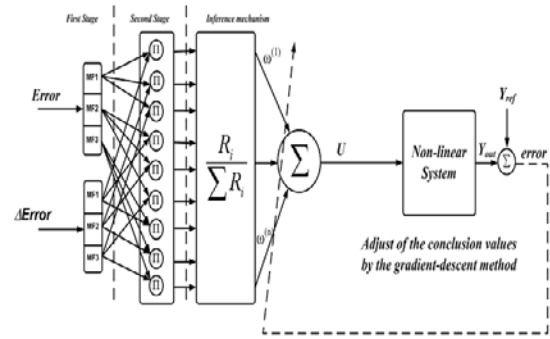


Fig.7 : The neuro-fuzzy scheme

The neuro-fuzzy calculation utilizes membership functions of gaussian kind. With Gaussian fuzzy sets, the algorithm is fit for using all data contained in the preparation set to calculate each rule conclusion, which is distinctive when utilizing triangular allotments. Fig.7 represents the neuro-fuzzy scheme for an illustration with two variables ( $x_1, x_2$ ) and one output variable ( $y$ ). In the principal phase of the neuro-fuzzy scheme, the two inputs are categorized into philological values by the set of Gaussian membership functions recognized to every variable. The second stage computes every tenet  $R^{(0)}$  its separate enactment degree. Last, the derivation system weights every guideline conclusion  $\omega^{(0)}$ , instated by the group based algorithm, utilizing the enactment degree computed in the second stage. As mentioned the error signal among the model inferred value  $Y$  and the particular measured value (or teaching value)  $y'$ , is employed by the gradient descent scheme to regulate each rule conclusion. Also he algorithm adjusts the values of  $\omega^{(0)}$  to diminish an objective function  $E$  typically expressed by the mean quadratic error (12). In this equation, the value  $y'(k)$  is the preferred output value correlated with the condition vector  $x'(k) = (x_1', x_2', \dots, x_m')$ . The element  $Y(x'(k))$  is the conditional response to the same condition vector  $x'(k)$  and calculated by Eq. (14).

$$E = \frac{1}{2} [Y(x(k)) - y(k)]^2 \\ Y(x'(k)) = \frac{\sum_{l=1}^c \left( \prod_{j=1}^m \mu_{A_j^{(l)}}(x_j'(k)) \right) \omega^{(l)}(k)}{\sum_{l=1}^c \left( \prod_{j=1}^m \mu_{A_j^{(l)}}(x_j'(k)) \right)} \quad (14)$$

Eq. (15) establishes adjustment for every conclusion  $\omega^{(0)}$  with the aid of gradient-descent method. Here the symbol  $\alpha$  is the learning rate parameter, and also  $t$  designates the number of learning iterations that are executed by the algorithm.

$$\omega^{(l)}(t+1) = \omega^{(l)}(t) - \alpha \frac{\partial E}{\partial \omega^{(l)}} \quad (15)$$

The inference function Eq. (14) depends on  $\omega^{(l)}$  only through its numerator. The expression composing the numerator is now represented by 'a' and is shown in Eq.(16).

$$a = \sum_{l=1}^c \left( \prod_{j=1}^m \mu_{A_j^{(l)}}(x'_j(k)) \right) \omega^{(l)}(k) \quad (16)$$

The denominator of function Eq. (14) is dependent on a term  $d^{(l)}$ , defined in Eq. (17), and denoted by b in Eq. (18).

$$d^{(l)} = \prod_{j=1}^m \mu_{A_j^{(l)}}(x'_j(k)) \quad (17)$$

$$b = \sum_{l=1}^c (d^{(l)}) \quad (18)$$

In order to compute the adjustment of each conclusion value  $\omega^{(l)}$ , it is necessary to compute the variation of the objective function E,  $\partial E$ , in relative to the disparity that occurred in  $\omega^{(l)}$  in the anterior instant,  $\partial \omega^{(l)}$ . So by, using the chain rule to calculate  $\partial E / \partial \omega^{(l)}$  results in Eq.(19).

$$\frac{\partial E}{\partial \omega^{(l)}} = \frac{\partial E}{\partial Y} \frac{\partial Y}{\partial a} \frac{\partial a}{\partial \omega^{(l)}} \quad (19)$$

The utilization of chain rule searches for the term contained in E that is straight forwardly reliant on the quality to be balanced, i.e., the conclusion value  $\omega^{(l)}$ . Therefore, we can verify by chain Eq. (19) that it starts with E dependent of Y value, and it basically depends on  $\alpha$  term also finally, expression a is a function of  $\omega^{(l)}$ . Now after few moment, the alteration can be done for  $\omega^{(l)}$  and also be interpreted that is propotional to the error that is between the neuro-fuzzy model response and the supervising value, but it can be weighted by the influence of rule (1), indicated by  $d^{(l)}$ , to the final neuro-fuzzy inference.

$$\omega^{l}(t + 1) = \omega^{(l)}(t) - \alpha \frac{(Y(x'(k)-y'(k))d^{(l)})}{\sum_{l=1}^c (d^{(l)})} \quad (20)$$

Next, a convergence theorem has been developed to assurance the stability of particular learning algorithm employed for the above-mentioned FNN [10]. A Lyapanov energy function is defined as follows:

$$V_k = J_k = \frac{1}{2} E_k^2 \quad (21)$$

From Eq. (19), we can get

$$\Delta V = V_{k+1} - V_k = \frac{1}{2} (E_{k+1}^2 - E_k^2) \quad (22)$$

The error difference,  $\Delta E_k$ , can be defined as

$$\Delta E_k = E_{k+1} - E_k = \frac{\partial E_k}{\partial \omega} \Delta \omega \quad (23)$$

$$\Delta \omega = \omega_{k+1} - \omega_k = -\alpha E_k \frac{\partial E_k}{\partial \omega} \quad (24)$$

Using Eq. (22), we can get

$$\begin{aligned} \Delta V &= \frac{1}{2} (E_{k+1} - E_k)(E_{k+1} + E_k) \\ &= \frac{1}{2} (\Delta E_k)(2E_k + \Delta E_k) \end{aligned} \quad (25)$$

Substituting eq. (24) into eq. (23), we have:

$$\begin{aligned} \Delta V &= \frac{1}{2} \frac{\partial E_k}{\partial \omega} \alpha E_k \frac{\partial E_k}{\partial \omega} (-2E_k + \frac{\partial E_k}{\partial \omega} \alpha E_k \frac{\partial E_k}{\partial \omega}) \\ &= \frac{1}{2} (E_k \frac{\partial E_k}{\partial \omega})^2 [(\frac{\partial E_k}{\partial \omega})^2 \alpha^2 - 2\alpha] \end{aligned} \quad (26)$$

If  $\Delta V < 0$ , the convergence of the algorithm described in eq.(26) can be guaranteed. Therefore, we have:

$$(\frac{\partial E_k}{\partial \omega})^2 \alpha^2 - 2\alpha < 0 \quad (27)$$

From eq. (27), we can obtain:

$$0 < \alpha < \frac{2}{(\frac{\partial E_k}{\partial \omega})^2} \quad (28)$$

## V. SIMULATION RESULTS

To evaluate the viability of the proposed control strategy, the system is simulated in SIMULINK/SIMPOWER for a period of 100sec of real and reactive load profiles.

Table 1: Hybrid distributed generation system parameters.

PEMFC Parameters	Values
Faraday's Constant	96487000 C/kmol
Hydrogen time constant( $t_{H_2}$ )	26.1 sec
Hydrogen valve molar constant( $K_{H_2}$ )	$8.43 \times 10^{-4}$
Kr Constant= $N_0/4F$	$9.9497 \times 10^{-7}$
No load voltage ( $E_0$ )	0.6V
Number of cells ( $N_0$ )	384
Oxygen time constant ( $t_{O_2}$ )	2.91 sec
Battery Model parameters	Values
Maximum allowable terminal voltage	730 V
Minimum allowable terminal voltage	710 V
Operating Terminal Voltage	725 V

SOC, %	70
<b>DC/AC Converter Parameters</b>	
Nominal AC Voltage	400 V
Nominal Phase Current	125 A
Nominal DC Voltage	720 V
R <sub>s</sub>	0.9 mΩ
L <sub>s</sub>	0.01mH
F <sub>s</sub> (Hz)	50 Hz
<b>DC/DC Converter Parameters</b>	
Rated Voltage ( V)	200/650V
Resistance (R)	2.3Ω
Rated Power	50KW
Capacitance (C)	1.5 mf
Inductor (L)	415 μH

The decision of the DC- bus voltage depends on the output voltage of the inverter required which must provide the grid voltage. The association among the DC link voltage  $V_{dc}$  and the line-to-line RMS grid voltage  $V_{LL,AC}$ , where  $m_a$  is the modulation index in the linear region, is specified in Eq. (29) [9].

$$V_{dc} \geq \frac{1.633}{m_a} V_{LL,AC} + \text{voltage drops} \quad (29)$$

The proposed control strategies are realized using MATLAB/SIMULINK environment by means of the parameters given in Table. 1 [5].

In order to show the response of the power control strategy during the unbalanced voltage condition, another simulation results have been extracted. In this case, The proposed control strategy has been inspected in case of unbalanced voltage conditions. An unbalanced voltage, resulting from unbalanced load, is applied at the grid side. The unbalanced voltage starts at 1.2 sec for duration of 2 sec. The grid voltage during unbalanced voltage has been shown in Fig.8.

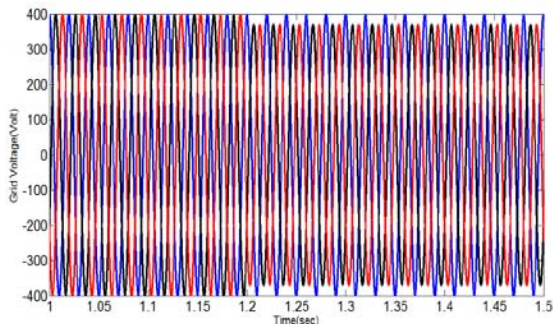


Fig.8 : The unbalanced grid voltages

Fig. 9 shows the 3-phase voltages; which are well regulated under the unbalanced disturbance.

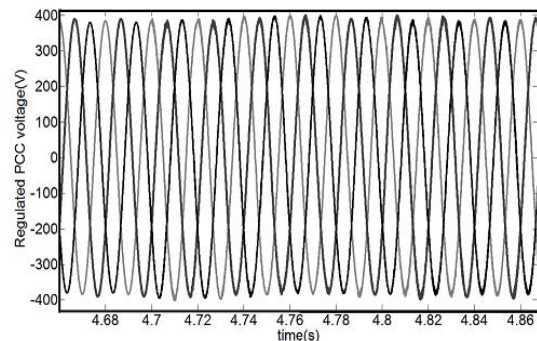


Fig.9 : Regulated grid voltage

From Fig.10 and Fig.11 the grid voltage and currents under the neuro-fuzzy controller have great improvement in case of Total harmonic distortion THD that was depicted in Fig.12.

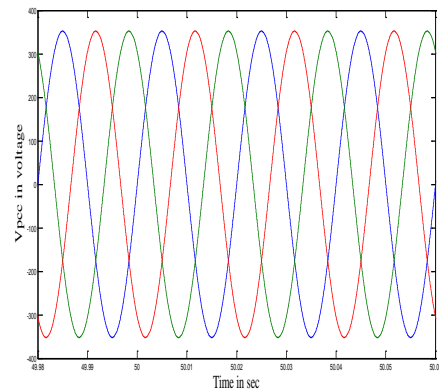


Fig. 10

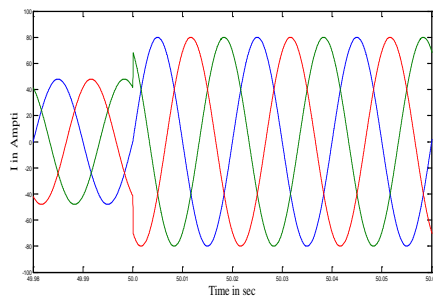


Fig. 11

From Fig.12 THD is only 3% in case of neuro-fuzzy controller and 15.27% in case of without neuro-fuzzy controller.

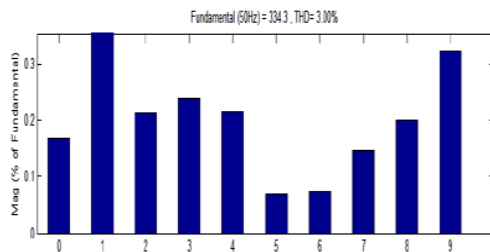


Fig. 12

The DC link voltage is shown in Figs.13. During the unbalanced voltage, there is an increase on DC link voltage but it is not much more than 10% of nominal value. In these conditions, to stabilize the dc-link power, the neuro-fuzzy controller manages the power flow between power sources.

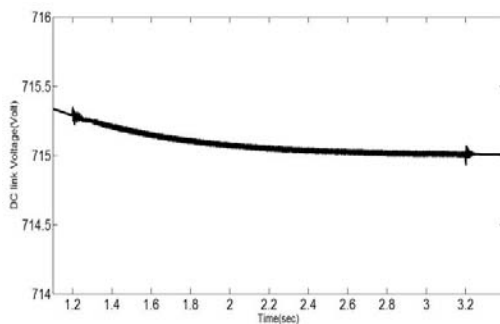


Fig.13: DC-link voltage

## VI. CONCLUSION

This paper presents modeling, control and power control in a grid connected PV/Fuel Cell/Battery hybrid power generation system in a microgrid. Here SIMULINK/SIMPOWER was utilized to model the system and simulate a power flow control strategy. PV, fuel cell and battery subsystems with power electronic converters are modeled. In addition, to disseminate the power between power sources, the neuro-fuzzy power controller has been produced to settle the DC-link power. Our simulation results are shown to exhibit the viability and ability of proposed control strategy amid various operating conditions in utility grid.

## REFERENCES RÉFÉRENCES REFERENCIAS

- Edward J. Coster, Johanna M. A. Myrzik, Bas Kruimer, Wil L.Kling, "Integration issues of distributed generation in distribution grids" proceedings of IEEE, January 2011.
- Djamila Rekioua and Ernest Matagne, "Optimization of Photovoltaic Power Systems", Springer, 2012
- M. Hashem Nehrir and C. Wang, "Modelling and Control of Fuel Cells", Wiley, 2009.
- C. M. Shepherd, "Design of primary and secondary cells II. Anequation describing battery discharge", J. Electrochem. Soc. 112,657 (1965).
- Amin Hajizadeh, Samson G. Tesfahunegn, and Tore M. Undeland, "Intelligent control of hybrid photo voltaic/fuel cell/energy storage power generation system" J. Renewable Sustainable Energy 3,043112 (2011); doi: 10.1063/1.3618743.
- Hussein K., Muta I., Hoshino T. and Osakada M., "Maximum photovoltaic power tracking: an algorithm for rapidly changing atmospheric conditions", IEE Journal of Generation, Transmission and Distribution, Vol. 142, pp. 59,1995.
- Yuri B., Shtessel Y. B., Zinober A. and Shkolnikov A., "Sliding mode control of boostand buck-boost power converters using method of stable system centre", Automatica, Vol. 39, pp.1061-1067, 2005.
- Hajizadeh A. and Golkar M. A., "Intelligent Robust Control of Hybrid Distributed Generation System under Voltage Sag", Journal of Expert Systems with Applications, Vol. 37, pp. 7627-7638, 2010.
- Mohan N., Undeland T.M. and Robbins W.P., Power Electronics Converters, Applications and Design, Wiley, 2003.
- Noroozian R., Abedi M., Gharehpetian G. B. and Hosseini S. H., "Operation of Stand Alone PV Generating System for Supplying Unbalanced AC Loads", *Iranian Journal of Electrical & Electronic Engineering (IJEED)*, Vol. 3, pp. 98-115, 2007.

This page is intentionally left blank